Q. J. R. Meteorol. Soc. (1995), **121**, pp. 187–210 551.556.44:551.510.534:551.509.313.2

Three-dimensional tracer initialization and general diagnostics using equivalent PV latitude–potential-temperature coordinates

By D. J. LARY[1]*, M. P. CHIPPERFIELD[1], J. A. PYLE[1], W. A. NORTON[2] and L. P. RIISHØJGAARD[3]

[1] *Cambridge University, UK*
[2] *Oxford University, UK*
[3] *Danish Meteorological Institute, Denmark*

(Received 6 January 1994; revised 15 June 1994)

SUMMARY

This paper describes a simple, but effective, procedure for producing three-dimensional tracer fields and general diagnostics based on an equivalent PV latitude–potential-temperature coordinate system. The tracer fields generated by this method are shown to agree quantitatively with independently measured profiles and total columns. Using this initialization makes short model simulations of around a week or so much more realistic. It can be used to assimilate non-global measurements, such as sonde or solar-occultation satellite data, or to transform two-dimensional model data into three-dimensional fields.

1. INTRODUCTION

For short-period numerical-model simulations of stratospheric ozone to be realistic, it is important to start the model from suitable initial conditions. The meteorological analyses prepared daily by various weather centres provide three-dimensional temperature and wind fields. Unfortunately, global data-sets for all the chemical tracers which need to be included in numerical models are not currently available. To try to overcome this limitation, this paper describes a simple, but effective, method for generating suitable initial tracer fields if the meteorological situation is known. The method was developed for use in the recent European Arctic stratospheric ozone experiment (EASOE) campaign and enables tracer fields taken from one meteorological situation (or a numerical model) to be used in initializing a three-dimensional model under a different meteorological situation. The process involves mapping tracer fields into a potential-vorticity (PV) equivalent latitude (ϕ_e)–potential temperature (θ) space and will be referred to as 'equivalent PV latitude initialization' (ELI). It uses many already well-established ideas related to the 'modified Langrangian mean' view of the atmosphere, and for the first time, produces a consistent tracer initialization which accounts for both the dynamical and photochemical states of the atmosphere. The method uses one coherent principle to reconstruct tracer fields; it also reduces 'spin-up' effects at the start of three-dimensional model simulations, since it generates tracer fields which are consistent with the physical and photochemical state of the atmosphere.

2. UNDERLYING PRINCIPLES

Under adiabatic conditions air parcels move along isentropic surfaces (surfaces of constant potential temperature, θ). Consequently, if tracer fields from one meteorological situation are to be used in initializing a model under different meteorological situations, it is very useful to have θ as a vertical coordinate, since it acknowledges the likely motion of air parcels. In addition, McIntyre and Palmer (1983, 1984), Hoskins *et al.* (1985) and Hoskins (1991) have shown the usefulness of isentropic maps of Ertel's potential vorticity in visualizing large-scale dynamical processes. Potential vorticity plays a central role in

* Corresponding author: Centre for Atmospheric Sciences, Department of Chemistry, Cambridge University, Lensfield Road, Cambridge, CB2 1EW, UK.

large-scale dynamics where it behaves as an approximate material tracer (Hoskins *et al.* 1985). As a result, potential vorticity can be used as the horizontal spatial coordinate instead of latitude and longitude (cf. Norton 1994), so reducing the tracer field from three dimensions to two. PV is sufficiently monotonic in latitude on an isentropic surface to act as a useful replacement coordinate. These ideas have already led to many interesting studies correlating potential vorticity and chemical tracers such as nitrous oxide and ozone (Schoeberl *et al.* 1989; Proffitt *et al.* 1989, 1993; Lait *et al.* 1990; Douglass *et al.* 1990), as well as PV–θ studies of ozone loss (D. Lucic, personal communication; P. von der Gathen, personal communication; Proffitt *et al.* 1989, 1993; Atkinson 1993). A key result of these studies is that PV and ozone mixing ratios are correlated on isentropic surfaces in the lower stratosphere, as was first pointed out by Danielsen (1968). In this paper we take these now well-established ideas and develop them as a basis for a method, on the one hand, of tracer initialization which is consistent with the dynamical and photochemical state of the atmosphere, and, on the other hand, for diagnostics which are an alternative to zonal means. Since the absolute values of potential vorticity depend strongly upon height and the meteorological condition, it is useful to normalize the potential vorticity and use potential-vorticity equivalent latitude (ϕ_e) as the horizontal coordinate instead of potential vorticity itself. The quantity ϕ_e is calculated by considering the area enclosed within a given potential-vorticity contour on a given θ-surface. The ϕ_e assigned to every point on this potential-vorticity contour is the latitude of a latitude circle which encloses the same area as the potential-vorticity contour. Therefore, for every level in the atmosphere, ϕ_e has the same range of values from $-90°$ to $+90°$, so providing a vortex-tracking coordinate system. The technique therefore is similar in principle to the methods employed by Schoeberl and co-workers, but differs in one important respect, in that it uses equivalent PV latitude (ϕ_e) and not PV.

If tracer concentrations are mapped into a PV-θ space in one situation and then a second situation is considered for which we require to reconstruct a three-dimensional ozone field, given the PV and θ, then it is likely that the range of PV values will differ between the two situations. This means that the total amount of ozone in the reconstructed field will be different from the total amount of ozone in the initial data-set. The use of ϕ_e instead of potential vorticity ensures that the range of values of the tracer is the same for a given isentropic surface in both the initial data and the reconstructed field; this is a key step in the effectiveness of our method.

In this study the meteorological fields were those from analyses carried out by the European Centre for Medium-range Weather Forecasts (ECMWF). The initial tracer data-sets were taken from two sources: Firstly, nine days of ozone-sonde measurements from various sites in the northern hemisphere made during the EASOE campaign in early 1992 were used to construct a two-dimensional ϕ_e–θ ozone field. Secondly, ozone data for 11 January 1992 from the microwave limb sounder (MLS) on the upper-atmosphere research satellite were used to construct a two-dimensional ϕ_e–θ ozone field. Tracer fields from a numerical model, either two-dimensional or three-dimensional, were also used.

The initial tracer fields generated in this way might well have had the correct features and spatial gradients, but not the right magnitudes (i.e. the concentrations could have been too high or too low) if the initial tracer data were not suitable for the given meteorological situation. This is because the reconstructed field can only be as good as the initial data permit. If the initial tracer field is not completely suitable for the meteorological situation, for whatever reason, some other form of adjustment of the tracer field may be required (such as normalization to observed total columns). In this particular study, because the initial tracer data were suitable, no adjustment was necess-

ary. All the studies reported on here involved data, initializations and diagnostics for the month of January 1992. Had ozone data from, for example, January 1989 been used to produce an initialization for January 1992, then some adjustment might have been necessary.

The method for initializing tracer fields outlined so far is most suitable for those constituents which are long lived, i.e. whose concentrations are controlled mainly by atmospheric motions. Of course, in the case of the more reactive constituents, chemistry also has a very important role. The rates at which chemical reactions proceed depend on several factors, such as the local temperature, pressure, and radiation fields. If the temperature and radiation fields for the situation from which the model is to be started are significantly different from those which applied for the initial tracer data, then the way in which the shorter-lived species are partitioned by the ELI step that has just been described will be inappropriate. To overcome this difficulty, a further operation, referred to as chemical balancing, can be tried. This simply involves using the three-dimensional tracer and temperature fields to run a 'chemistry only' three-dimensional model for a short period of time, typically for the equivalent of one day. This allows a repartitioning of the reactive constituents to occur, consistent with the initial meteorological conditions, and also introduces features such as sharp gradients across the terminator for short-lived species like nitric oxide and nitrogen dioxide. By definition, this step has virtually no effect on long-lived tracers such as nitrous oxide, but it does have a large effect on the more reactive constituents.

It has been found that, when the approach just described is used, then subsequent numerical model integration does not undergo a dramatic initial 'spin-up' where there are rapid changes in many of the tracer fields. This means that short-term simulations initialized using ELI instead of the often-used zonally-symmetric initialization will be more realistic.

By storing tracer fields in ϕ_e–θ bins the correlation between any two can be found, and could be used to assess the effect of non-adiabatic processes on long-lived tracer concentrations (Butchart and Remsberg 1986) and the non-conservative effects on PV. Of course, in the case of the short-lived species we would not expect to find good correlations owing to the fact that the local temperature, pressure and radiation fields will have a large effect on the concentrations.

3. An initialization case-study

To assess the usefulness of the ELI method, a case-study was done in which completely independent data-sets could be used and then compared with each other in different ways. The ozone data that we used came from ozone sondes released at various sites across the northern hemisphere, and from the MLS, both used in conjunction with the ECMWF analyses, also from the total ozone mapping spectrometer (TOMS). The ECMWF and TOMS data were both on an approximately 5° by 5° latitude–longitude grid.

Several types of comparison were made. In the first all the data from ozone sondes released at various sites across the northern hemisphere between 1 and 9 January 1992 were used to construct the ϕ_e–θ ozone field which is shown in Fig. 1. Where sonde data were not available, generally at low PV values, a January ozone field from a two-dimensional model in isentropic coordinates (Harwood and Pyle 1977, 1980 adapted by Kinnersley and Harwood 1993) was used. This ϕ_e–θ ozone field (together with the ECMWF analyses for two days later) was used to generate a three-dimensional ozone field by ELI ('two days later' was chosen so that the ozone data used for the comparison

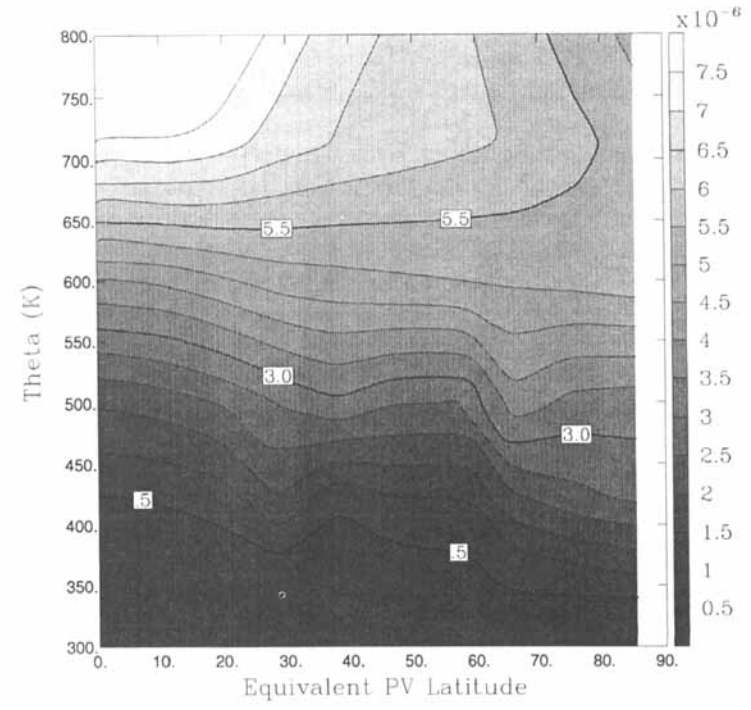

Figure 1. The ϕ_e–θ ozone field reconstructed from balloon sondes launched between 1 and 9 January 1992 together with ECMWF analyses. Where sonde data were unavailable a two-dimensional model ozone field was used. This accounts for the jagged contours for ϕ_e at around 40°.

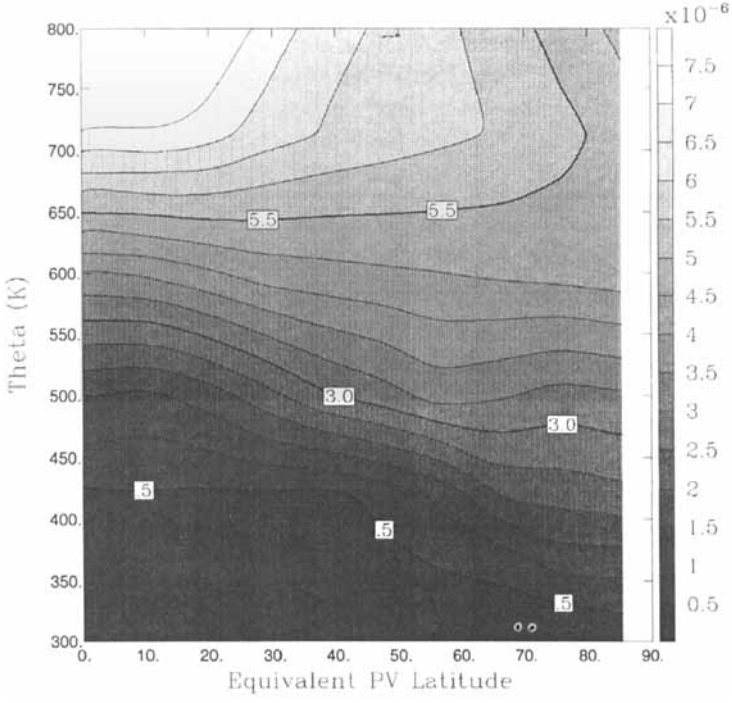

Figure 2. The ϕ_e–θ ozone field reconstructed from MLS ozone data for 11 January 1992 together with ECMWF analyses. Where MLS data were unavailable a two-dimensional model ozone field was used.

were not involved in the reconstruction). The same procedure was repeated for a second ϕ_e–θ ozone field constructed from the MLS measurements made on 11 January 1992 (Fig. 2). Vertical profiles through both of these reconstructed fields were then compared with the data from the sonde ascents (Figs. 3 to 5) and also with the TOMS total ozone column for 11 January 1992 (Fig. 6).

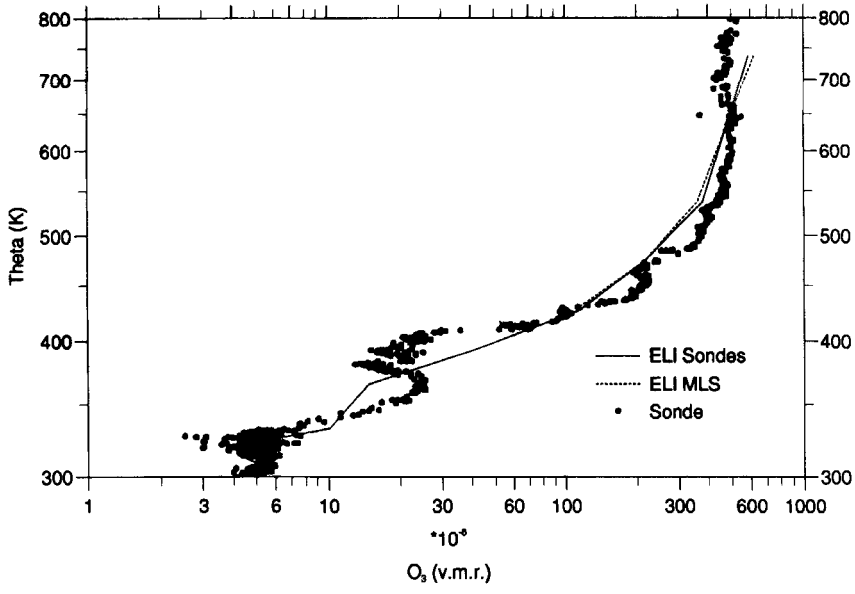

Figure 3. The vertical ozone profile above Aberystwyth (52.4°N, 4.1°W) on 11 January 1992 as measured by an ozone sonde (dots) and as reconstructed by ELI. Note how the MLS and sonde reconstructions almost overlie each other.

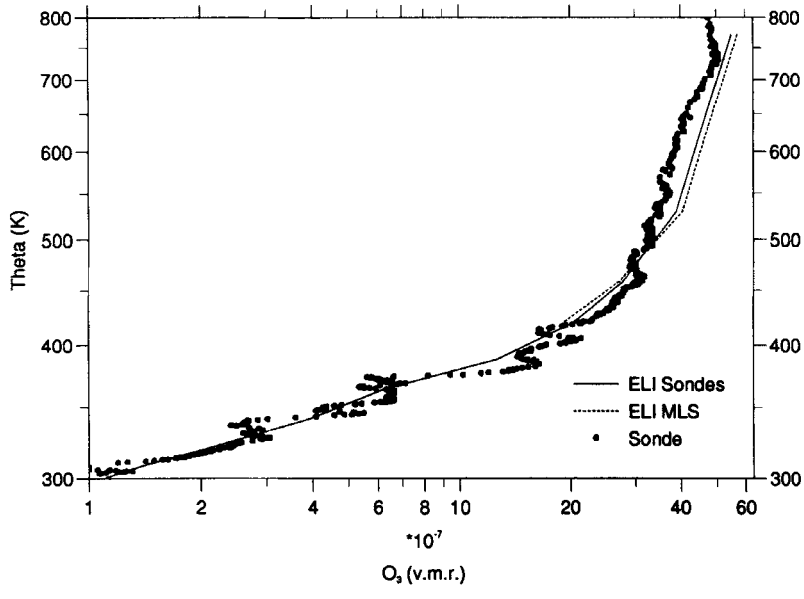

Figure 4. The vertical ozone profile above Esrange (67.9°N, 21.1°E) on 11 January 1992 as measured by an ozone sonde (dots) and as reconstructed by ELI. Note there is a different x-axis scale from Fig. 3.

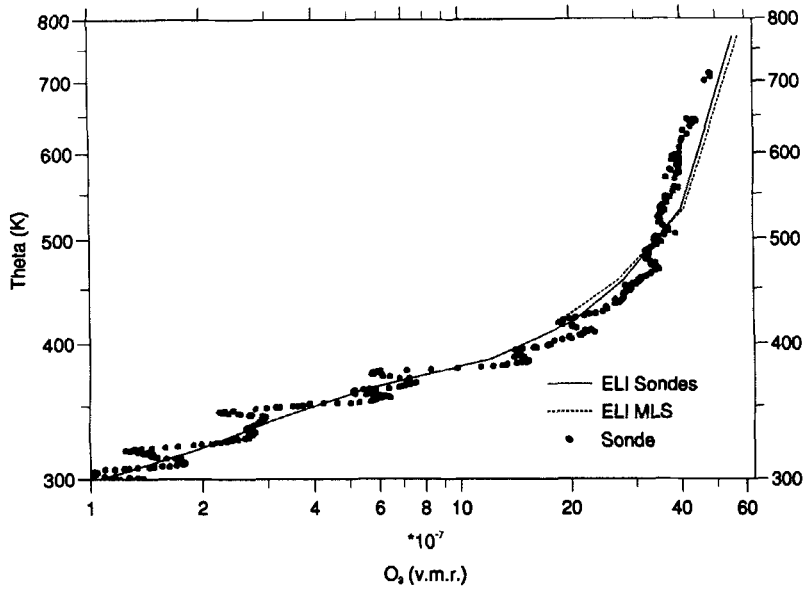

Figure 5. The vertical ozone profile above Sodankyla (67.4°N, 26.6°E) on 11 January 1992 as measured by an ozone sonde (dots) and as reconstructed by ELI.

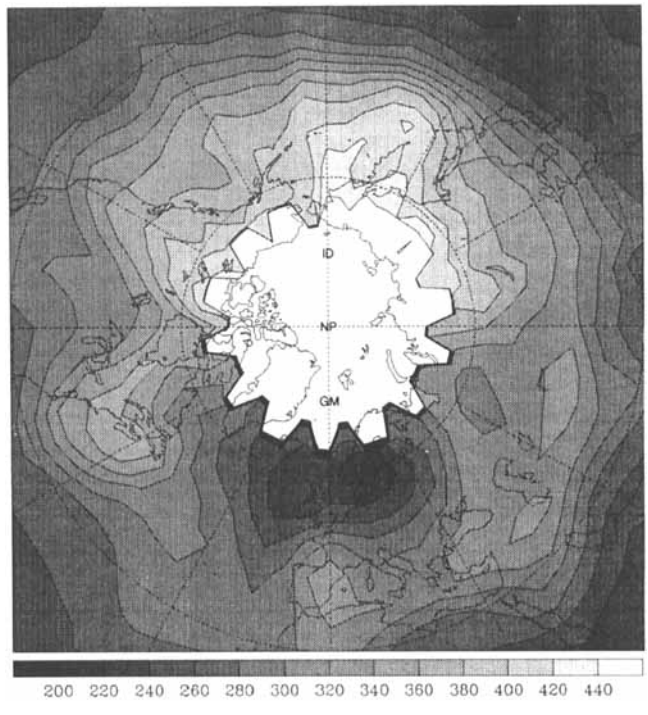

Figure 6. The total ozone field in Dobson units for 11 January 1992 on an approximately 5° by 5° latitude–longitude grid as seen by TOMS. GM refers to the Greenwich meridian. All subsequent polar stereographic plots have the same orientation.

Figures 1 and 2 show the ϕ_e–θ ozone fields constructed from sonde data and MLS data, respectively. As mentioned earlier, where data were unavailable a two-dimensional model ozone field was used, which accounts for the jagged contours at ϕ_e of around 40° in Fig. 1.

To provide a stringent test of the method it is important that the set of data used for the reconstruction of the ozone distribution is completely independent of that with which it is then compared.

(*a*) *Profile comparison*

Figures 3, 4 and 5 show comparisons for 11 January 1992 of sonde profiles for Aberystwyth, Esrange and Sodankyla, respectively, with reconstructed ELI profiles using the ϕ_e–θ ozone fields obtained from ozone sondes and from MLS. The profiles were chosen because they represented different meteorological conditions, although not that far apart in terms of latitude. Aberystwyth is well within the vortex, whereas Esrange and Sodankyla are not. This was apparent from the fact that the initialization using only θ was able to reproduce the profile for Esrange but not for Aberystwyth. The agreement between the reconstructions and the observations is good, particularly when it is remembered that the vertical resolution in use for the meteorological analyses was much less than that for the sondes. The comparatively low vertical resolution of the analyses meant that the reconstructed profiles could, at best, be a 'smoothed' version of the real sonde profiles. It is encouraging that the profiles reconstructed independently from MLS and the ozone sondes are also in good agreement with each other. Note that the MLS profiles are not shown below 400 K because the lowest MLS retrieval level is 100 mb and below this level MLS uses climatological data.

(*b*) *Column comparison*

Figure 6 shows the total ozone column as measured by TOMS (level 6) for 11 January 1992 averaged onto an approximately 5° by 5° latitude–longitude grid. This can be compared with the two ELI total ozone column fields which used MLS (Waters *et al.* 1993) and sonde data, respectively, shown in Figs. 7 and 8. The meteorological analyses was done by ECMWF for 12.0 GMT 11 January 1992. A comparison of those figures shows that there is qualitative agreement between the TOMS measurements and the ELI reconstructions in both the shape of the main features of the total ozone field and the magnitude of the total ozone column. For example, the pool of low ozone centred over northern Europe is well captured by the reconstruction, the minimum value in the TOMS field is 218.5 Dobson units with 226 Dobson units in both the ELI/MLS reconstruction and the ELI/sonde reconstruction. Also well reproduced by ELI is the ridge of high total ozone across the Aleutians and Canada.

A problem encountered during computation of the total ozone columns arose from the fact that the ECMWF analyses extends only up to 10 mb. So, when calculating the contribution to the total column from the highest level (10 mb), the ozone concentration had to be scaled by a factor of 0.7 to account for the fact that the ozone concentration above 10 mb is not constant, but rather decreases with height. The value 0.7 was arrived at by doing many sample calculations with complete ozone profiles. This factor will, in reality, change with location and time as the shape of the ozone profile evolves. Our calculations ought to be repeated using meteorological analyses which extend above 10 mb. Bearing in mind this limitation of the data currently available to us, we attempted to quantify the agreement between TOMS and the ELI reconstruction more precisely. Percentage differences were taken between the TOMS field and the two ELI reconstructions and are shown in Fig. 9 as a zonal average. In this particular case the

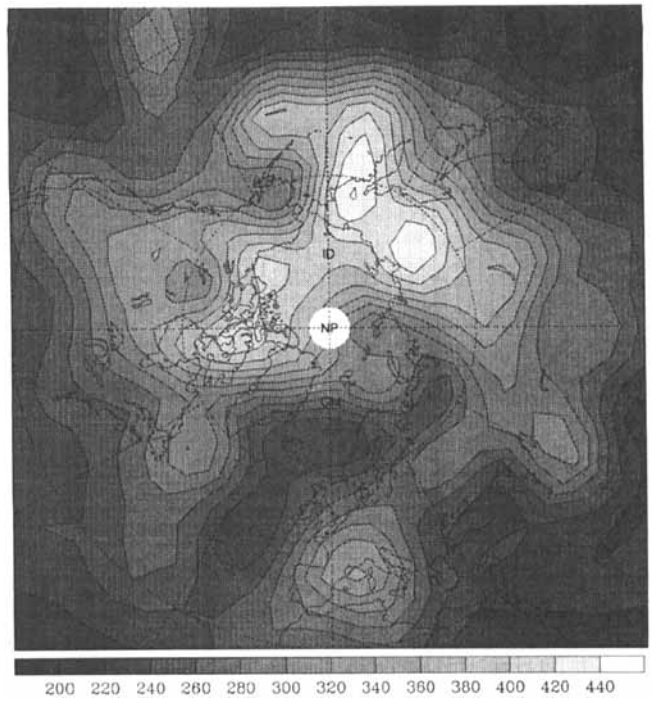

Figure 7. The total ozone field in Dobson units for 11 January 1992 on an approximately 5° by 5° latitude–longitude grid as reconstructed by an ELI MLS initialization.

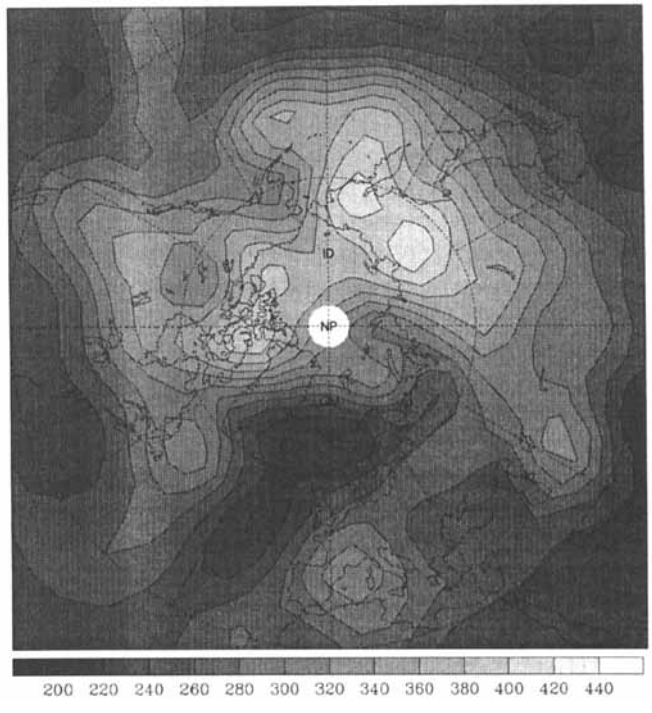

Figure 8. The total ozone field in Dobson units for 11 January 1992 on an approximately 5° by 5° latitude–longitude grid as reconstructed by an ELI sonde initialization.

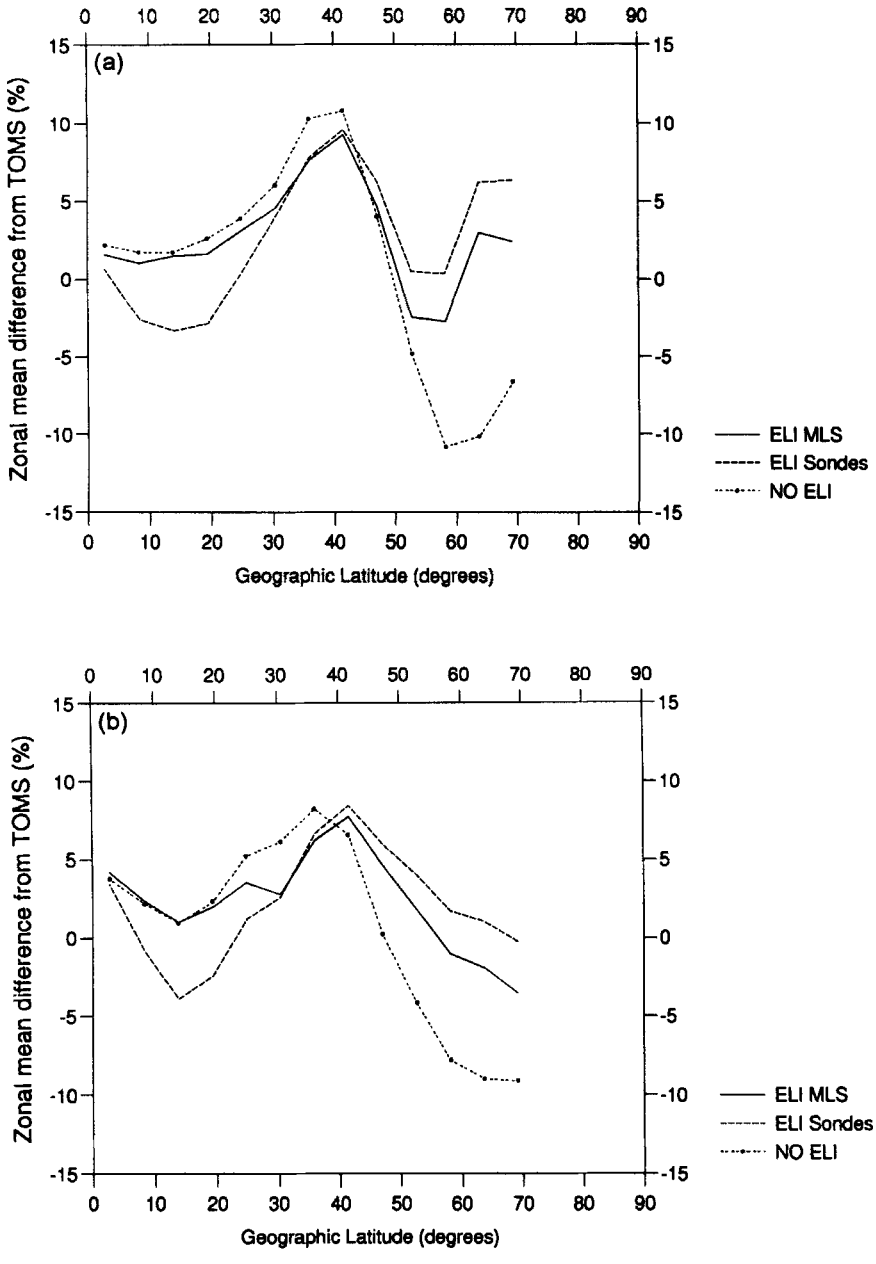

Figure 9. The zonal average percentage difference between the total ozone field in Dobson units as measured by TOMS and as reconstructed by ELI for (a) 11 January 1992, (b) 13 January 1992 and (c) 16 January 1992.

zonal average agreement is within 10%, which is probably comparable to the errors in measurement and those which occur because of differences in sampling time. TOMS data are taken near local noon while the reconstructions refer to 12 GMT. The agreement will obviously depend on the choice of the scale factor, and could probably be improved if analyses above 10 mb could be used so that scaling was not required. As is to be expected, when ELI is not used and, instead, a zonally symmetric initialization of ozone

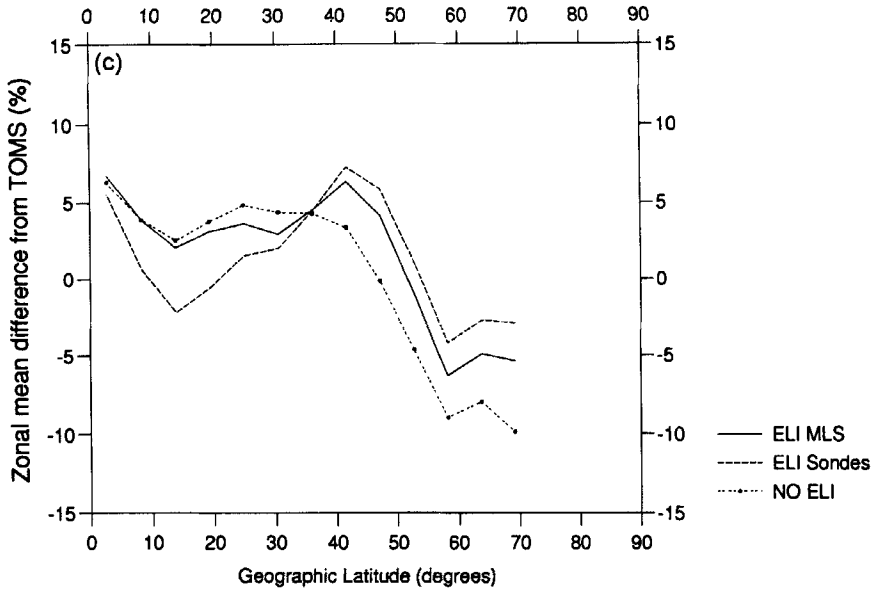

Figure 9. Continued.

on θ-surfaces is carried out (the curve marked NO ELI in Fig. 9), then the agreement with TOMS is not so good. This was so particularly at around latitude 60°N.

At lower latitudes there were only a few sondes launched during January 1992, and the data-sparse region was filled in by using a two-dimensional model ozone field. Differences between the sonde and MLS initialization were therefore greatest in this region (Fig. 9). In fact, a total of less than 25 sonde ascents were available for the initialization, which is why 9 days in January were used, thereby increasing the number of ascents. It is quite remarkable that with such a sparse ozone data-set we managed to achieve as much as we did. Clearly an initialization method will succeed in producing results that are only as good as the input data. However, these results show that, even with a relatively sparse data-set, our method was able to reconstruct a three-dimensional field. This is of particular value for measurements which do not have a global coverage, for example, sondes or satellite measurements that use solar occultation techniques.

4. THE ROLE OF θ AND ϕ_e

It has been known for some time that there is a correlation between the total ozone column and the height of the tropopause (see, for example, Dobson 1968 for an overview). Since potential vorticity is the product of absolute vorticity and static stability, air parcels will stretch or compress vertically as they enter regions of different vorticity (Price and Vaughan 1993). Consequently, high values of total ozone are to be expected in regions of high vorticity in the lower stratosphere (as the air parcels stretch vertically), and low values of total ozone in regions of low vorticity (as the air parcels compress vertically). Vaughan and Price (1991) showed that at least half the variance in total ozone on synoptic scales can be explained by changes in vorticity just above the tropopause.

Contributions from both θ and ϕ_e are required for the generation of a realistic tracer field. In an attempt to quantify the role of ϕ_e alone, the TOMS maps and ELI initializations in Figs. 6 to 8 were compared with a zonally symmetric initialization using MLS

ozone data on θ-surfaces. To do this the two-dimensional θ–ϕ_e ozone data-set from MLS was used, as in the ELI case, except that, this time, the equivalent PV latitude, ϕ_e, was replaced by the geographical latitude, ϕ (i.e. the vortex tracking coordinate was not used). The potential temperature, θ, was still used as the vertical coordinate to account for the vertical displacement of isentropic surfaces. This produced a zonally symmetric ozone field on isentropic surfaces. The total ozone field which resulted is shown in Fig. 10. The zonally symmetric initialization does capture the larger-scale 'wave one' feature, but the smaller-scale features are not reproduced as well as in the full ELI reconstructions shown in Figs. 7 and 8. In particular, the zonally symmetric initialization does not capture the low total ozone values present over the British Isles. The advantage of using ϕ_e as well as θ is that the effect of both the horizontal and vertical excursions of air are included.

When the vertical profiles are examined, the use of a zonally symmetric initialization on θ-surfaces, instead of the full ELI, changes the Aberystwyth profile significantly, particularly near the surface (Fig. 11). At this time Aberystwyth was in the pool of low total ozone over the British Isles. The Esrange and Sodankyla profiles are not affected to the same extent (Fig. 12). The fact that the profiles agree as well as they do for Esrange and Sodankyla, and that the gross features of the total ozone column were qualitatively reproduced when zonally symmetric initialization on θ-levels was used, shows the value of using θ as a vertical coordinate.

If the lower section of the Aberystwyth profile is enlarged (Fig. 11(b)), i.e. the region where the meteorological analyses have a much higher vertical resolution, the success of ELI can be seen more clearly. It should again be mentioned that the reconstructed profile did not include the data with which it had been compared; the two data-sets are independent of each other.

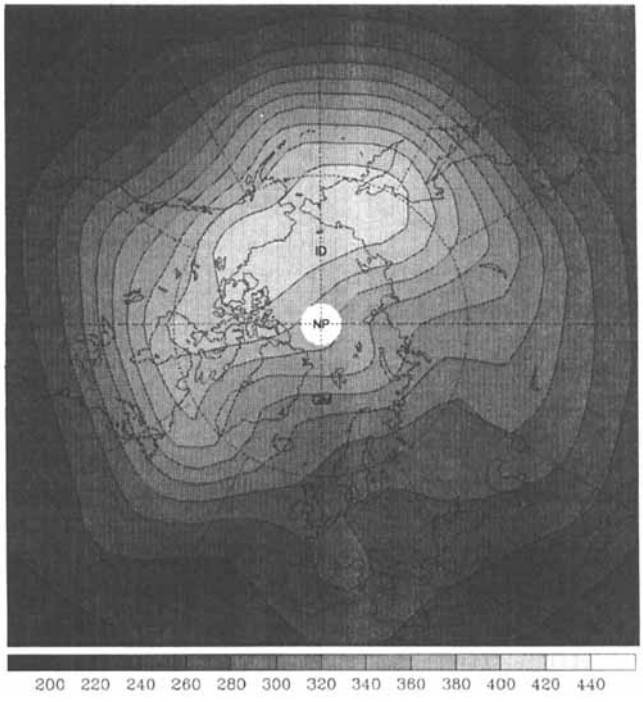

Figure 10. The total ozone field in Dobson units for 11 January 1992 on an approximately 5° by 5° latitude–longitude grid as reconstructed by a zonally symmetric initialization of ozone on θ-levels.

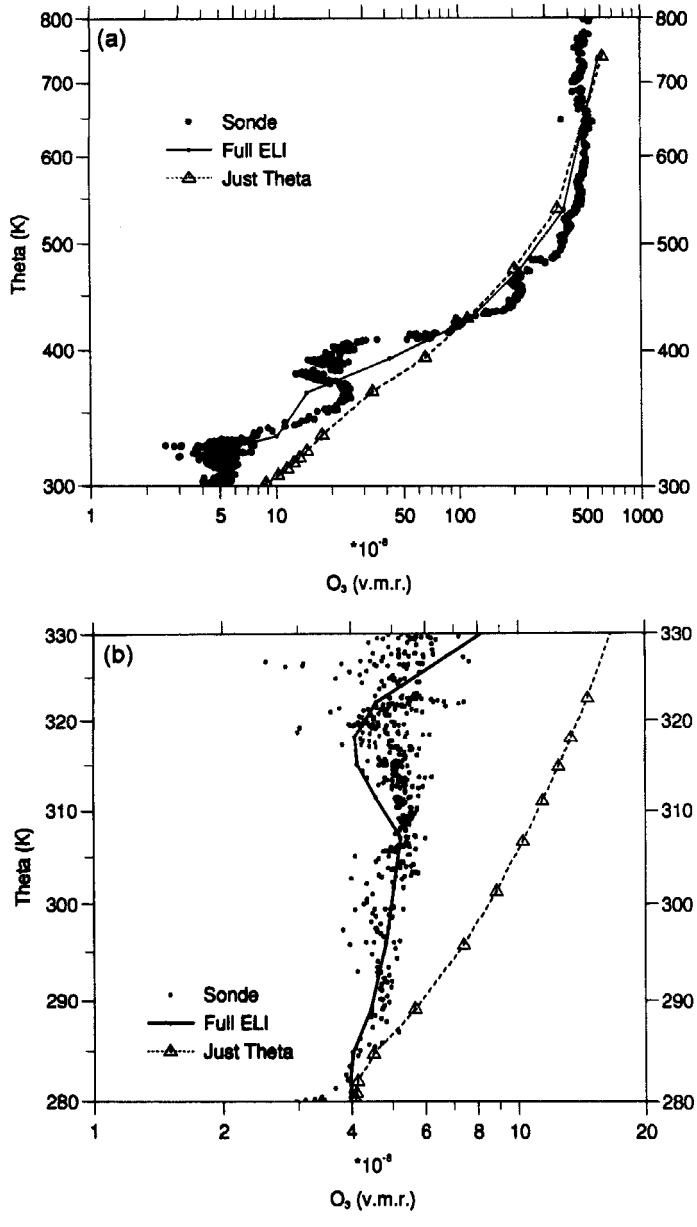

Figure 11. (a) The vertical ozone profile above Aberystwyth (52.4°N, 4.1°W) on 11 January 1992 as measured by an ozone sonde (dots) and as reconstructed by ELI (solid line) and a zonally symmetric initialization on θ-surfaces (dashed line). (b) An enlargement of the lower section of the vertical ozone profile above Aberystwyth.

5. Effect of ELI on numerical model 'spin up'

To show how ELI can reduce the model 'spin-up', three model simulations were performed using the initial ozone fields shown in Fig. 7 (MLS with ELI), Fig. 8 (sondes with ELI) and Fig. 10 (MLS without ELI), all without any chemical balancing. Each simulation lasted for the equivalent of only five days. Five days is, typically, a period

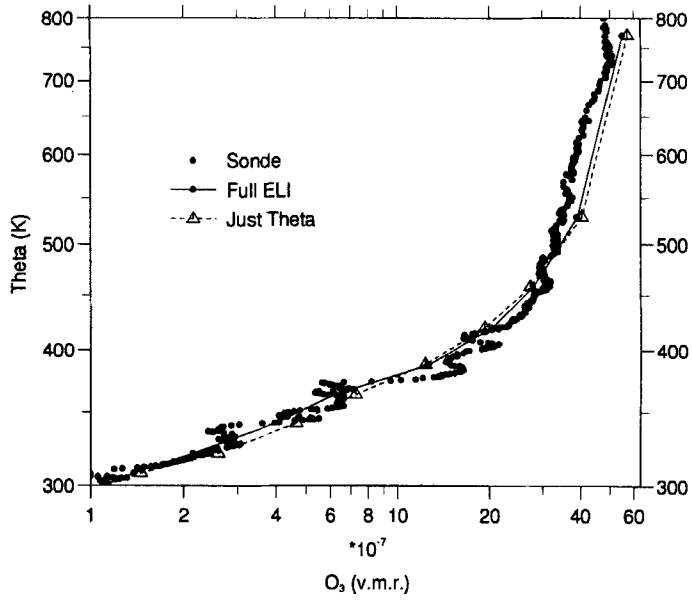

Figure 12. The vertical ozone profile above Esrange (67.9°N, 21.1°E) on 11 January 1992 as measured by an ozone sonde (dots) and as reconstructed by ELI and a zonally symmetric initialization on θ-surfaces.

during which the stratospheric forecast of the model remains realistic (see for example Carver *et al.* 1994). After five days any comparison between a simulation and TOMS is likely to be not so good because of the quality of the forecast. Figure 13 shows the results of the simulations compared with the column observed by TOMS. Figure 9 shows the zonally averaged difference between the simulated total ozone column and that observed by TOMS. It can be seen that the initial differences (Fig. 9(a)) between the zonally symmetric initialization and TOMS are considerably reduced after five days (Fig. 9(c)). Figure 13 shows that, in terms of the total ozone column, the simulation which started from the zonally symmetric initialization seems to have 'spun up', so that after five days of simulation all three simulations produced total ozone columns which are very similar.

The similarity between the total ozone columns is not necessarily reflected so well in the concentration fields at all levels. For example, Fig. 14 shows the 10 mb ozone field simulated in two runs, with and without ELI. In the zonally symmetric run (right-hand column) the lowest ozone concentrations are initially placed over the pole. The strong cross-polar jet then almost cuts this pool of low ozone in half and after five days the ozone field resembles a horseshoe with a large ozone minimum just east of the Aleutians. In the ELI run (left-hand column) the lowest ozone values were initially offset from the pole towards the European side of the hemisphere. Relatively high concentrations of ozone were placed quite close to the pole along latitude 180°E with a second pool of high ozone at the position 45°N, 120°E. These initial conditions mean that after five days the secondary ozone minimum east of the Aleutians was not as large in the ELI run as in the zonally symmetric run. In the ELI run the ozone-rich air which was close to the pole and also at position 70°N, 60°E has been moved by the cross-polar jet to give a pool of high ozone close to position 50°N, 240°E. This is not present to the same extent in the zonally symmetric initialization, instead the pool of low ozone is almost cut in half. Clearly, a good agreement between the total ozone column and TOMS does not necessarily mean that the model ozone field at all levels will be as realistic as the total column.

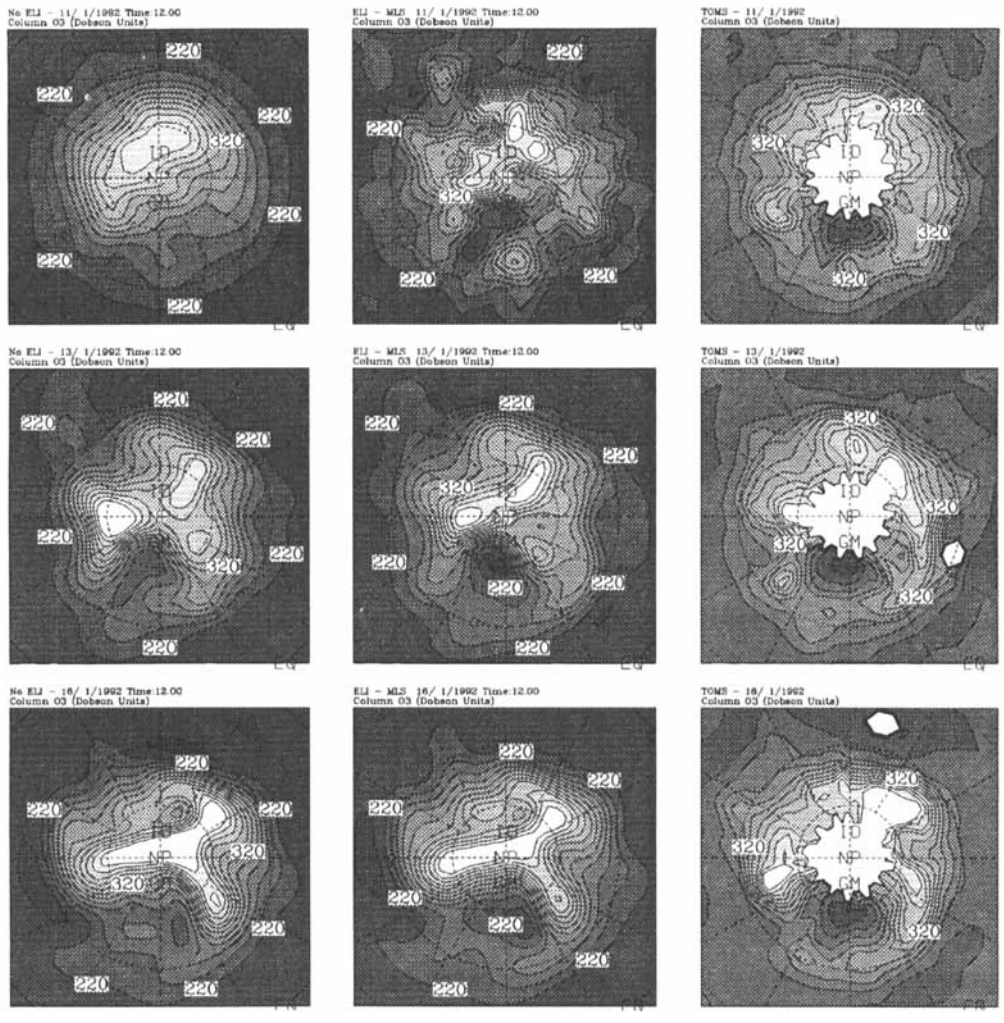

Figure 13. The total ozone field in Dobson units for three days in January 1992 on an approximately 5° by 5° latitude–longitude grid for a three-dimensional model simulation starting from a zonally symmetric initialization of ozone on θ-surfaces (left-hand column), for a three-dimensional model simulation starting from an ELI/MLS initialization of ozone (centre column), and the total column observed by TOMS (right-hand column). The plots are oriented so that the Greenwich meridian (marked GM) is vertical.

It probably represents a good agreement in the region close to the tropopause, which as mentioned earlier, is important for determining the total ozone column. In addition, it should be noted that the 'spin-up' time required for a model which starts from a zonally symmetric initialization will vary with altitude and with the prevailing meteorological conditions.

To summarize, a zonally symmetric initialization of ozone on isentropic levels will capture the large-scale features of the ozone field qualitatively, but a full ELI initialization is much better, particularly for the first few days of a simulation. This was clearly demonstrated by examining vertical ozone profiles. A zonally symmetric initialization was able to reproduce some vertical profiles reasonably well while not capturing others. For example, the Esrange profile was reproduced quite well, but the Aberystwyth profile, which was associated with a blocking anticyclone, was not well reproduced by a zonally symmetric initialization but was well reproduced by ELI.

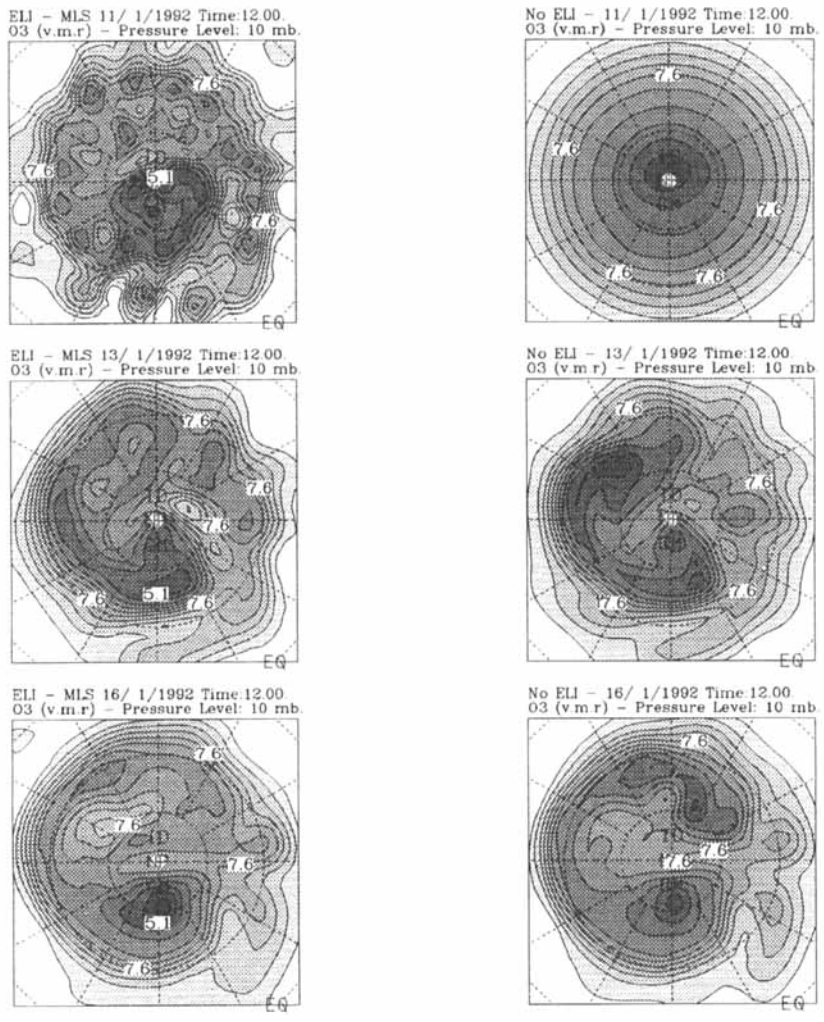

Figure 14. The ozone volume mixing ratio (ppmv) at 10 mb for three days in January 1992 for a three-dimensional model simulation starting from an ELI/MLS initialization of ozone (left-hand column) and for a three-dimensional model simulation starting from a zonally symmetric initialization of ozone on θ-surfaces (right-hand column). The highly structured appearance of the initial field constructed by ELI is a reflection of the PV analysis. The latitude and longitude lines are shown every 30°. The plots are oriented so that the Greenwich meridian (marked GM) is vertical.

6. Using a ϕ_e–θ coordinate system for general diagnostics

Tracer initialization is just one of many possible applications for a ϕ_e–θ coordinate system. This form of coordinate system is also useful for general meteorological diagnostics. When conducting climatological studies the zonal means of many different variables are often taken. However, around the latitude circles where these zonal means are formed there can often be large variations, particularly during periods when the dynamics is far from zonal in nature. In such cases part of the zonal mean will relate to air inside the vortex and part to air outside the vortex. A coordinate system which acknowledges that a strongly asymmetric vortex is present would in these circumstances be an advance over using a zonal mean, and at least would offer an important complementary view.

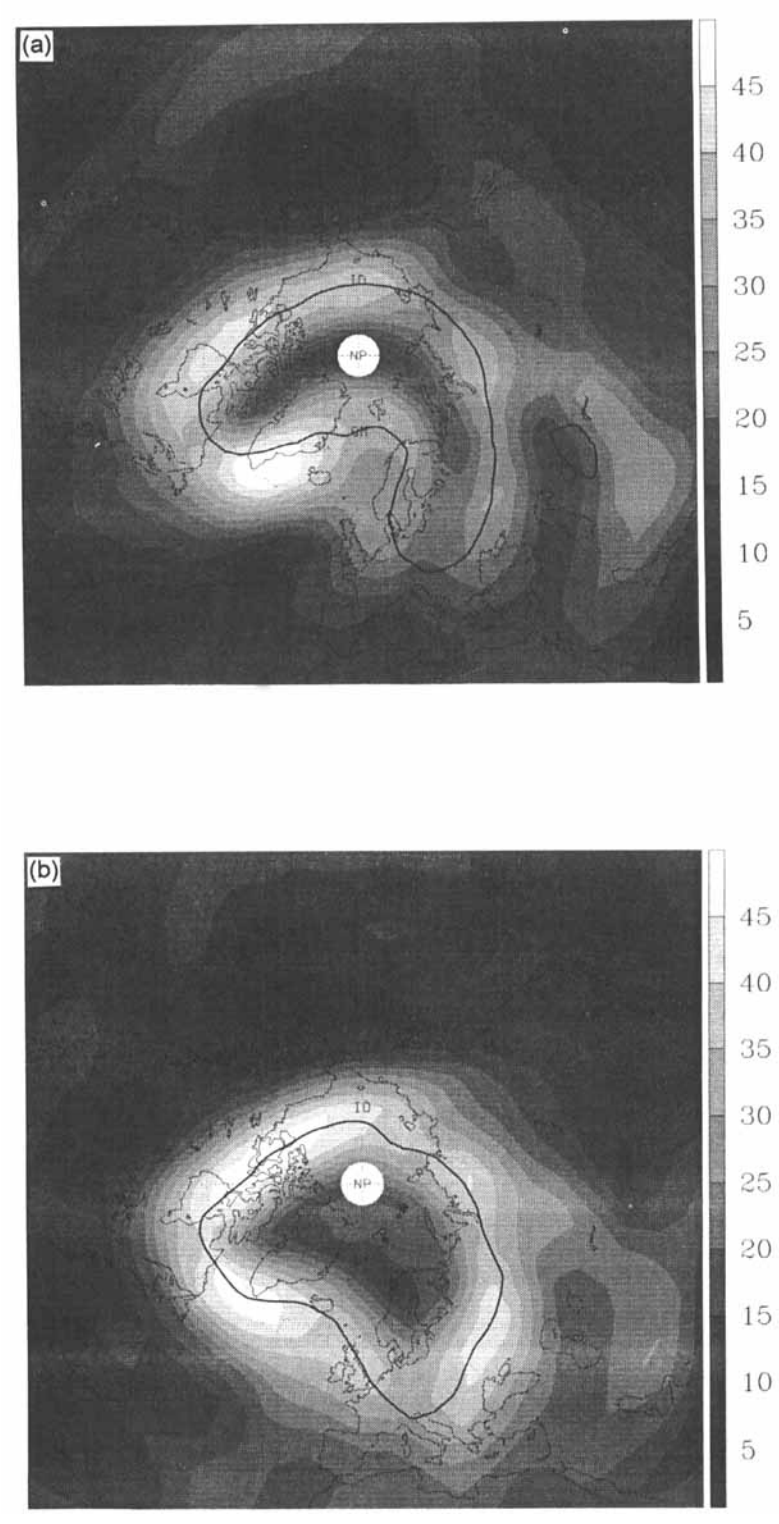

Figure 15. The wind speed for 27 January 1992 from the ECMWF analyses overlaid with the 65° ϕ_e-contour, (a) for $\theta = 500$ K, (b) for $\theta = 700$ K.

In this section we look at the ϕ_e means (the mean around contours of constant ϕ_e) for two variables—wind speed and temperature. This analysis we refer to as 'equivalent PV latitude analysis' (ELA).

(*a*) *Wind speed*

We would expect ELA to be particularly useful for wind speed, because, for example, the polar vortex could be defined either in terms of wind speed (the location of the jetstream) or in terms of PV. The useful property of ϕ_e is that, unlike PV, it is not a strong function of height. Figure 15 shows the wind speed on the 500 K and 700 K isentropic surfaces for 27 January 1992 overlaid with a single 65° ϕ_e-contour. Although the vortex has quite different shapes on the different isentropic surfaces, the 65° ϕ_e-contour is still a good estimate of the 'middle' of the vortex edge since on that day it generally transected the region of highest wind speeds for each level in the analyses above about 450 K. The vertical cross-section of wind speed (Fig. 16) shows that on that day the highest wind speeds (or vortex edge) lay between ϕ_e-contours of approximately 60° to 70° for all levels above the 450 K surface. Below the 450 K surface there is no distinct vortex. Although there is no obvious reason why this is so, it was found that for the winter of 1991/92 the same band of ϕ_e-contours (60°–70°) could be used to define the vortex for all levels throughout most of the winter.

For comparison with the ELA cross-section shown in Fig. 16, Fig. 17 shows the zonal-mean cross-section for the same day. As the vortex was far from zonal, particularly at around 500 K, the zonal mean can at best provide a 'smoothed' view. By contrast, the ELA cross-section clearly depicts how tight and fast the circumpolar jet was, in a way that the zonal mean could not. In the ELA cross-section the jet centre is around 20° from a ϕ_e of 90°, whereas in the zonal mean the jet is shown as wider and, at the upper levels, extending polewards of 80°N to less than 10° from the pole.

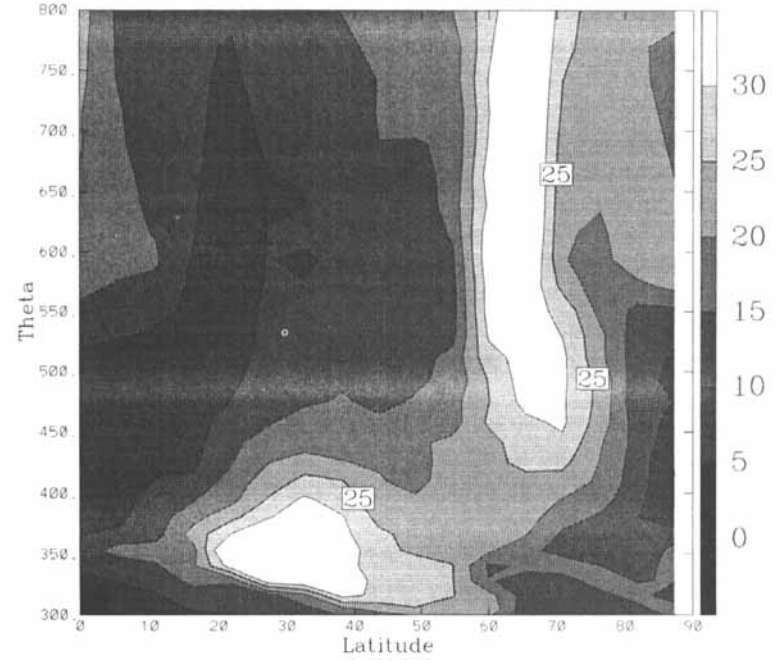

Figure 16. The ELA mean of the wind speed for 27 January 1992 (contours from 0 to 30 by 5).

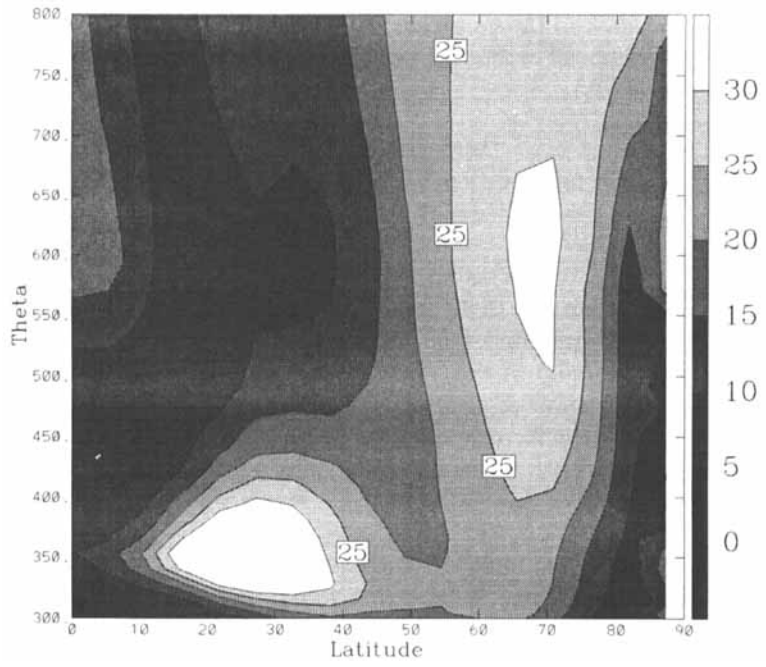

Figure 17. The zonal mean of the wind speed for 27 January 1992 (contours from 0 to 30 by 5).

(*b*) *Temperature*

Unlike wind speed, temperature is not always well correlated with PV. During periods when an undisturbed vortex exists the lowest temperatures may tend to be in the centre of the vortex but this is often not the case when a perturbed vortex is present. Figure 18 shows the temperature on the 500 K and 700 K isentropic surfaces for 27 January 1992 overlaid with a single 65° ϕ_e-contour (as in the previous section). On the 700 K surface the vortex edge encounters the highest and lowest temperatures for that isentropic level as air rises over the blocking anticyclone centred over northern Europe and then descends over Russia. Lower down on the 500 K surface, the temperature contours are almost parallel to the 65° ϕ_e-contour for a large portion of the vortex edge.

When the vertical cross-sections are examined in Figs. 19 and 20, the zonal mean shows the −50 °C contour at 700 K extending up to 80°N with a lowest temperature of around −70 °C. On the other hand, the ELA cross-section shows the −50 °C contour at 700 K at a much lower latitude (approximately 60°N) with a much larger region enclosed by the −60 °C contour than in the zonal mean cross-section. For this particular day the largest difference between the ELA and the zonal-mean sections was above 550 K. Below 550 K and at low latitudes there were few differences between the two analyses.

To summarize, ϕ_e is found to be particularly useful for defining a vortex edge. In the 1991/92 winter the same range of ϕ_e-contours (60°–70°) could be used to define the centre of the vortex edge for many isentropic levels and for a considerable length of time. The ELA vertical wind speed cross-section clearly shows a faster and tighter jet than the zonal-mean analysis. The ϕ_e–θ coordinate system evidently tracks the vortex well whereas the zonal mean does not. For the day in question the ELA vertical temperature cross-section was qualitatively very similar to the zonal mean, but above 550 K showed that a larger region of the atmosphere was experiencing low temperatures

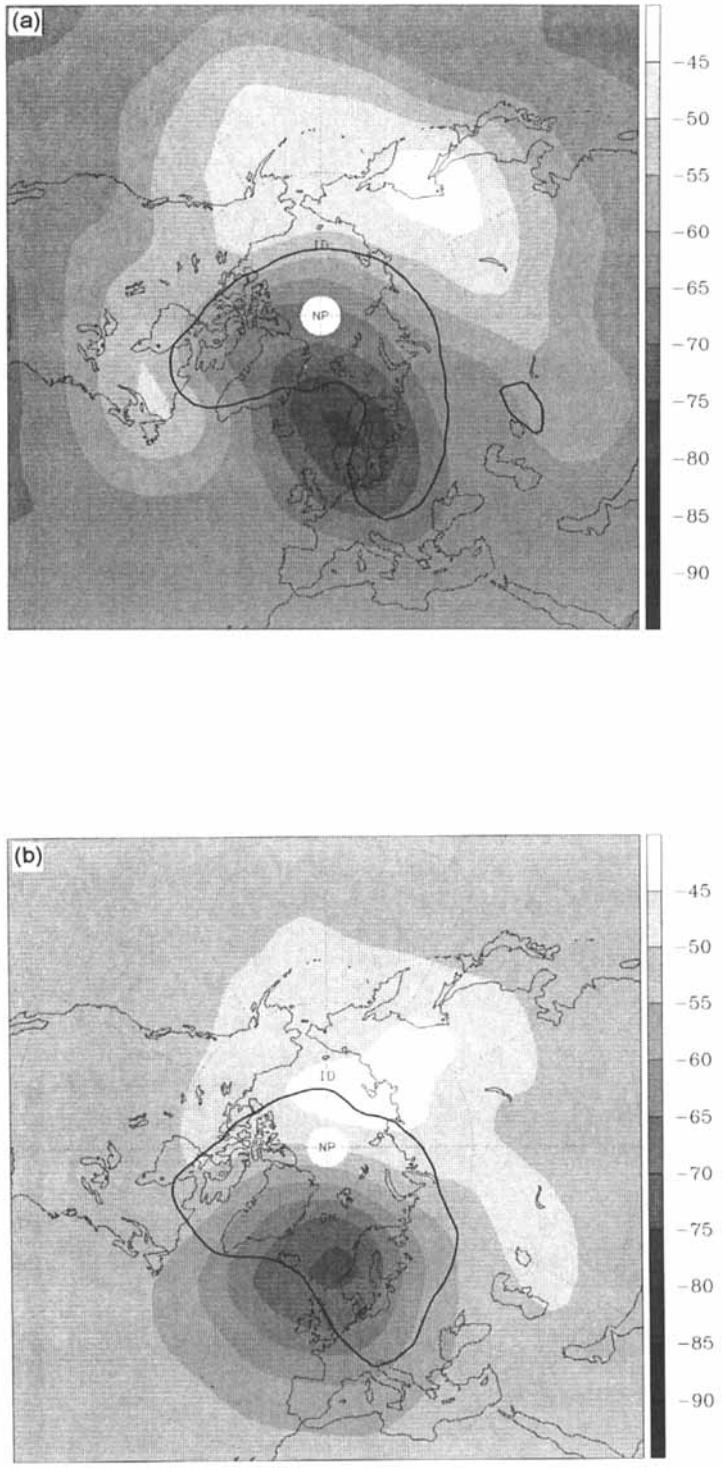

Figure 18. The temperature for 27 January 1992 from the ECMWF analyses overlaid with the 65° ϕ_e-contour, (a) for $\theta = 500$ K, (b) for $\theta = 700$ K.

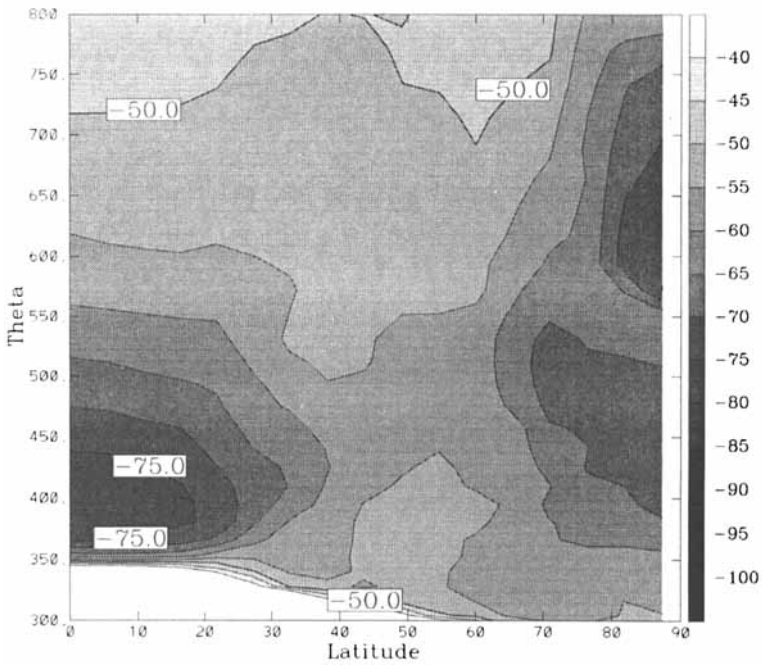

Figure 19. The ELA mean of temperature for 27 January 1992 (contours from −100 to −40 by 5).

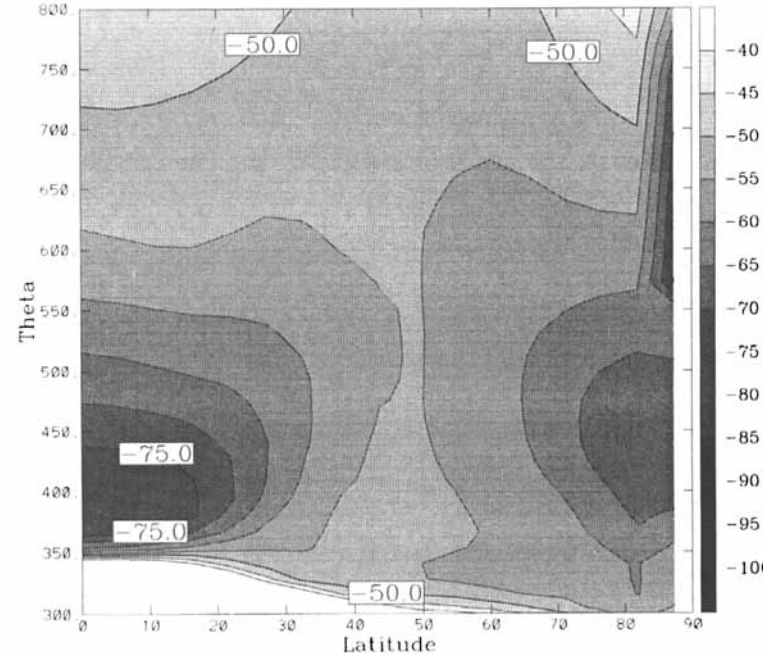

Figure 20. The zonal mean of temperature for 27 January 1992 (contours from −100 to −40 by 5).

than was apparent in the zonal-mean plot. On this occasion, and very often, temperature in the stratosphere at high latitudes correlates better with PV than with latitude.

(*b*) *Further diagnostics*

It is our intention to carry out a further study in which the standard deviation of measured tracer concentrations in a given ϕ_e–θ bin are used as a quantitative measure of how well tracers such as nitrous oxide are correlated with ϕ_e (or PV), and, more particularly, to highlight regions and times of year where the correlation is not good. Such regions are likely to be interesting as they could be regions with strong diabatic effects on PV. The spread of values in a given ϕ_e–θ bin could therefore be used as a measure of the non-conservation of PV by processes such as irreversible mixing.

7. Conclusions

The ϕ_e–θ coordinate system has been shown to be generally useful for applications such as tracer initialization and diagnostics since it accounts explicitly for the gross meteorological features of a given situation.

An effective initialization procedure, called ELI, has been described which aims to use information about the dynamical state of the atmosphere to determine suitable initial tracer distributions for a general circulation model. The spatial gradients produced by this method and those deduced from satellite and sonde observations are in good agreement. Since the method is based upon the ϕ_e–θ coordinate system it is quite general and could be used to help assimilate tracer data-sets provided from various instruments such as, for example, those on the upper-atmosphere research satellite (UARS). It could also be used to assimilate measurements which do not have global coverage, such as those from sondes or the solar occultation satellite measurements. Another benefit of the method is that it reduces 'spin-up' effects which are often encountered at the start of the model simulation, since it starts from conditions which are dynamically consistent with the state of the atmosphere (even if not correct). This initialization is now being used in our chemical modelling studies associated with the UK universities global atmospheric modelling programme (UGAMP). From a case-study of 11 January 1992 the method has been shown to agree quantitatively with three completely independent data-sets and has captured both the observed horizontal and vertical gradients in the ozone distribution quite well.

A ϕ_e–θ coordinate system can also be used for other applications such as meteorological diagnostics where ϕ_e means give a useful complementary picture to that provided by zonal means when the flow is far from zonal. Such an analysis was referred to as equivalent PV latitude analysis (ELA). In addition, the spread of values in a given ϕ_e–θ bin could itself be used as a useful diagnostic.

Acknowledgements

The Centre for Atmospheric Science is a joint initiative of the Department of Chemistry and the Department of Applied Mathematics and Theoretical Physics. This work forms part of the Natural Environmental Research Council (NERC) UK universities global atmospheric modelling programme. It was partly supported by grant STP0016 from DGXII and STEP-CT91-0139 of the Commission for the European Committees (CEC). DJL thanks M. E. McIntyre for many useful conversations, and G. C. Carver, J. Kettleborough and J. Stringer for their technical help. We thank Joe Waters and

Lucien Froidevaux of the Jet Propulsion Laboratory for kindly providing us with the MLS data used in this study. Ozone sonde data was obtained during the EASOE campaign, funded by the DGXII of the CEC. The data was obtained from the NILU data-base, we thank Geir Braathan for the excellent provision of this data facility. We also thank the ECMWF for making their analyses available to us, and R. D. McPeters, A. J. Krueger (NASA/GSFC) for the TOMS data used in this study, also S. J. Reid, A. Howells, U. Schmidt and Esko Kyro for the use of their sonde data. WAN was supported by a grant from NERC under the British Antarctic Survey (BAS) special topic.

APPENDIX

Calculation of equivalent PV latitude, ϕ_e

The PV is first put onto a set of isentropic levels and the area within the PV contours on each isentropic level is then calculated. This is done by finding the range of PV values which are present on the given θ-level and then constructing a set of PV 'bins' which cover this range of PV values. Each latitude–longitude gridpoint on the θ-level is then scanned to see which PV bin it is in, and the area of the current grid square is added to the cumulative total area of that bin. When this process has been completed the area enclosed by each PV contour is known. This area can then be easily converted into an equivalent latitude, ϕ_e (see below). Care in choosing the number of PV bins is needed. If too few are chosen satisfactory results will not be obtained owing to the lack of resolution. In this study 180 PV bins were used.

The area of a grid square can be calculated using simple geometry. The area of a spherical cap from a latitude ϕ up to the pole is given by the equation

$$A_{\text{cap}} = 2\pi r^2\{1 - \cos(90 - \phi)\} \tag{1}$$

and so the area enclosed by a latitude belt, A_{belt}, between two latitudes in the same hemisphere ϕ_1 and ϕ_2, enclosing areas $A_{\text{cap}1}$ and $A_{\text{cap}2}$, is given by

$$A_{\text{belt}} = |A_{\text{cap}1} - A_{\text{cap}2}| \tag{2}$$

Note, that if the equator is crossed then the latitude belt should be split up into two belts of ϕ_1 to 0°, and 0° to ϕ_2. So the area of a rectangular cell whose width in degrees of longitude is $\Delta\lambda$ is given by

$$A_{\text{cell}} = \frac{\Delta\lambda}{360} A_{\text{belt}} \tag{3}$$

Alternatively, if we have an area A we can convert this to an equivalent latitude by using the expression

$$\phi_e = \sin^{-1}\left(1 - \frac{A}{2\pi r^2}\right) \tag{4}$$

Figure A.1 shows an example of such a calculation made using the ECMWF analysis for 6 January 1992 (initially at T 106 but truncated to T 21). On the 476 K isentropic levels the 'surf zone' of McIntyre and Palmer (1984) can be seen where there is a relatively weak large-scale gradient of potential vorticity (close to bin 100 in Fig. A.1; note that a small change in area between adjacent bins is associated with strong PV gradients, and a large change in area between bins is associated with weak gradients). This surrounds the edge of the polar vortex which has steeper potential vorticity gradients (approximately between bins 120 and 160 in Fig. A.1). Then within the vortex, bins 165 to 180, there is

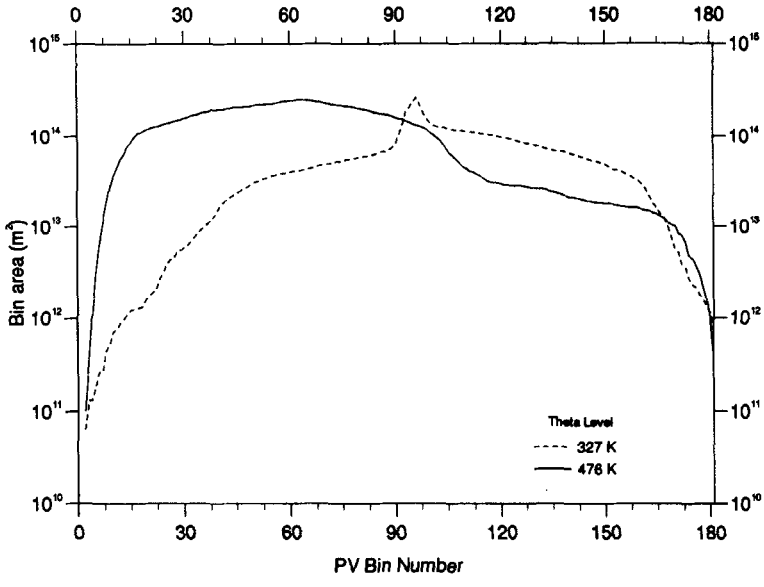

Figure A.1. The area enclosed by a PV contour which falls within a given PV bin for different isentropic levels. For each isentropic level there are 180 PV bins which cover the range of PV values found on that isentropic level. The maximum area should always be that of a hemisphere. Note that this plot includes both hemispheres; the maximum area enclosed in a PV interval corresponds to the PV contour enclosing the same area as a hemisphere.

a weaker PV gradient. The peak in area at all levels occurs for the PV contour which encloses the same area as a hemisphere (approximately 2.55×10^{14} m^2).

If the input tracer data-set is three-dimensional then this procedure needs to be repeated twice, once for the meteorological analysis relevant to the input data (this then allows the tracer concentrations to be put into bins and a ϕ_e–θ tracer field to be generated) and another time for the meteorological analysis for which initial tracer fields are required so that each three-dimensional gridpoint can be assigned a tracer value.

REFERENCES

Atkinson, R. J. 1993 'An observational study of the Austral spring stratosphere: Dynamics, ozone transport and the ozone dilution effect'. PhD thesis, Massachusetts Institute of Technology

Butchart, N. and Remsberg, E. E. 1986 The area of the stratospheric polar vortex as a diagnostic for tracer transport on an isentropic surface. *J. Atmos. Sci.*, **43**, 1319–1339

Carver, G. D., Norton, W. A. and Pyle, J. A. 1994 A case study in forecasting the stratospheric vortex during EASOE. *Geophys. Res. Lett.*, **21**, 1451–1454

Danielsen, E. F. 1968 Stratospheric-tropospheric exchange based on radioactivity, ozone and potential vorticity. *J. Atmos. Sci.*, **25**, 502–518

Dobson, A. R. 1968 *Exploring the atmosphere*. Clarendon Press, Oxford

Douglass, A. R., Rood, R. B., Stolarski, R. S., Schoeberl, M. R., Proffitt, M. H., Margitan, J. J., Loewenstein, M., Podske, J. R. and Strahan, S. E. 1990 Global three-dimensional constituent fields derived from profile data. *Geophys. Res. Lett.*, **17**, (4), 525–528

Lait, L. R., Schoeberl, M. R., Newman, P. A., Proffitt, M. H., Loewenstein, M., Podolske, J. R., Strahan, S. E., Chan, K. R., Gary, B., Margitan, J. J., Browell, E., McCormic, M. P. and Torres, A.	1990	Reconstruction of O_3 and N_2O fields from ER-2, DC-8, and balloon observations. *Geophys. Res. Lett.*, **17,** (4), 521–524
Harwood, R. S. and Pyle, J. A.	1977	Studies of the ozone budget using a zonal-mean circulation model and linearized photochemistry. *Q. J. R. Meteorol. Soc.*, **103,** 319–343
	1980	The dynamical behaviour of a two-dimensional model of the stratosphere. *Q. J. R. Meteorol. Soc.*, **106,** 395–420
Hoskins, B. J.	1991	Toward a PV-theta view of the general circulation. *Tellus*, **A43,** 27–35
Hoskins, B. J., McIntyre, M. E. and Robertson, A. W.	1985	On the use and significance of isentropic potential vorticity maps. *Q. J. R. Meteorol. Soc.*, **111,** 877–946
Kinnersley, J. S. and Harwood, R. S.	1993	An isentropic two-dimensional model with an interactive parametrization of dynamical and chemical planetary-wave fluxes. *Q. J. R. Meteorol. Soc.*, **119,** 1167–1194
McIntyre, M. E. and Palmer, T. N.	1983	Breaking planetary waves in the stratosphere. *Nature*, **305,** 593–600
	1984	The 'surf zone' in the stratosphere. *J. Atmos. Terr. Phys.*, **46,** 825–849
Norton, W. A.	1994	Breaking Rossby waves in a model stratosphere diagnosed by a vortex-following technique for advecting material contours. *J. Atmos. Sci.*, **51,** 654–673
Price, J. D. and Vaughan, G.	1993	The potential for stratosphere–troposphere exchange in cut-off-low systems. *Q. J. R. Meteorol. Soc.*, **119,** (510), 343–365
Profitt, M. H., Steinkamp, M. J., Powell, J. A., McLaughlin, R. J., Mills, O. A., Schmeltekopf, A. L., Thompson, T. L., Tuck, A. F., Tyler, T., Winkler, R. H. and Chen, K. R.	1989	*In situ* ozone measurements within the 1987 Antarctic ozone hole from a high-altitude ER-2 aircraft. *J. Geophys. Res.*, **94,** (ND14), 16 547–16 555
Proffitt, M. H., Atkin, K., Margitan, J. J., Loewenstein, M., Podolske, J. R., Weaver, A., Chan, K. R., Fast, H. and Elkins, J. W.	1993	Ozone loss inside the northern polar vortex during the 1991–1992 winter. *Science*, **261,** (5125), 1150–1154
Schoeberl, M. R., Lait, L. R., Newman, P. A., Martin, R. L., Proffitt, M. H., Hartman, D. L., Loewenstein, M., Podolske, J., Strahan, S. E., Anderson, J., Chan, K. R. and Gary, B.	1989	Reconstruction of the constituent distribution and trends from ER-2 flight observations. *J. Geophys. Res.*, **94,** 16 815–16 845
Vaughan, G. and Price, J. D.	1991	On the relation between total ozone and meteorology. *Q. J. R. Meteorol. Soc.*, **117,** 1281–1298
Waters, J. W., Froidevaux, L., Read, W. G., Manney, G. L., Elson, L. S., Flower, D. A., Jarnot, R. F. and Harwood, R. S.	1993	Stratospheric ClO and ozone from the Microwave Limb Sounder on the Upper-Atmosphere Research Satellite. *Nature*, **362,** (6421), 597–602